Cyber-physical Integrated Planning of Distribution Networks Considering Spatial-temporal Flexible Resources

Shutan Wu, Qi Wang, Qichao Chen, Changping Yu, and Yi Tang

***Abstract*—The rapid development of cyber technology and the increase of flexible resources have transformed the distribution network into a cyber-physical distribution system, while the accompanying multidimensional uncertainties have brought new planning challenges. In this paper, an innovative approach is proposed to effectively leverage distributed resources while considering the impact of cyber-physical coupling in distribution network planning. A cyber-physical integrated planning model of the distribution network is proposed, considering the effects of spatial-temporal flexible resources and multi-network coupling. Specifically, a three-layer optimization model is established and analyzed by the simulate anneal-particle swarm optimization algorithm. The upper layer achieves the optimization of the location and configuration of energy storage systems and smart terminal units. The middle layer optimizes the data load migration strategy using spatial-temporal flexible resources to solve the voltage exceeding problem caused by high penetration of distributed power access, while the lower layer optimizes the cyber side communication topology, improving the convergence speed and control performance of the distribution network. Then, the optimization model is analyzed iteratively with objective functions including total planning cost, operation excess loss and distributed control performance. Finally, the effectiveness and economy of the proposed planning scheme is verified and compared to traditional methods.**

***Index Terms*—Cyber-physical distribution system, distributed resources, integrated planning model, spatial-temporal migration.**

I. Introduction

With the increasing demand for electricity and push for energy transition, traditional distribution systems have undergone significant development. The high penetration of distributed generation (DG) into distribution systems with randomness and volatility poses challenges to the safety and reliability of the systems [1]–[2]. In the meantime, the access of flexible resources such as energy storage and demand response (DR) resources enriches the operation and regulation ability of distribution networks [3]–[4]. In terms of network integration, the monitoring, measurement, decision-making and control processes of distribution systems are highly dependent on high-speed and reliable communication networks, whereas the construction of high-energy-consuming digital infrastructures such as data centers and base stations makes the computation network highly coupled with the power network. Thus, traditional distribution networks have been transformed into cyber physical distribution systems (CPDS) [5], [6]. With the changes and challenges brought by the abovementioned emerging subjects, it is necessary to reconsider distribution network planning work from the perspective of cyber-physical coupling. In comparison to traditional distribution network planning, the methodology of CPDS planning differs in terms of the planning objects and optimization algorithms.

With respect to planning objects, many existing distribution network planning methods have considered the cooperative allocation of network resources to enhance the efficiency of distributed resource utilization and maximize economic benefits. In the newly built distribution network planning stage, equipment investment costs and expected operational effects are usually considered based on various uncertainties, and thus a multi-objective optimization model including economy, reliability and stability indicators can be established. In [7] and [8], coordinated planning methods for distribution networks with DG siting and network construction schemes are proposed, considering the uncertainties of loads and DGs. In the expansion planning stage, multiple types of physical equipment, e.g., DG [9], energy storage systems (ESSs) [10], grouping and switching capacitors [11], soft open points (SOPs) [12], static reactive power compensation devices [13], and new schedulable load resources [14], are configured, to improve the efficiency of system operation and delay

Received: June 26, 2023
Accepted: November 2, 2023
Published Online: May 1, 2024
Qi Wang (corresponding author) is with the School of Electrical Engineering, Southeast University, Nanjing 210096, China (e-mail: wangqi@seu.edu.cn).
DOI: 10.23919/PCMP.2023.000316

network investment. In [15] and [16], an optimal network expansion and energy storage configuration scheme is proposed to accommodate high proportions of photovoltaic and new load access, thus reducing the cost of network expansion and adapting to the uncertain development of distributed power sources and loads.

With respect to optimization models and solving algorithms, a multi-layer architecture including multiple evaluation index levels is usually established to consider planning and operational stages simultaneously, and appropriate mathematical solution methods or artificial intelligence (AI) algorithms are selected according to accuracy and time requirements [17]–[19]. In [17], a joint planning problem of ESS and DG considering operational constraints is solved through a two-layer optimization architecture to determine the optimal siting and capacity of different adjustable resources. The minimal total cost is selected as an economic objective in the upper layer, while the power supply interruption time and load curtailment loss are considered the reliability objectives in the lower layer. An AI algorithm is adopted to realize the iteration solution between the two layers.

Nevertheless, the abovementioned planning methods are mainly focused on the optimal allocation of multiple types of resources on the physical side, without involving information resources. The development of information and communication technology (ICT) has gradually enhanced the observability and controllability of CPDS [20]–[23], bringing changes to traditional distribution network planning, specifically in the two aspects described below.

The cyber-physical interaction capability is enhanced in CPDS. The coordination and optimization of distribution networks containing distributed resources depend on safe and reliable communication networks. Considering cyber-physical integration in the planning stage can meet the demand for efficient source-network-load interaction and enhance the availability maintenance ability of the distribution network. Research considering cyber-physical interaction has been carried out through communication networks and intelligent terminal planning. An integrated planning framework among distribution communication networks and distribution automation is proposed in [24], and coordination indices among them are studied. By considering the cyber-physical relationship, interactive and flexible operation of distribution network equipment is realized, and the economy of the distribution network under normal working condition is improved. A functional failure model considering information equipment is established in [25], and a distribution terminal planning model after considering the role of control functions is proposed. Ther has also been research on the communication network and communication terminal configuration from the perspective of output optimization and studies have proposed the optimal configuration scheme for distribution terminals to improve the reliability of the distribution network against failures. However, the above studies are based on the existing physical side planning scheme to expand the communication network and communication equipment, and the coupling effect of the physical side and cyber side needs to be further explored.

The flexibility of cyber resource regulation is increased in CPDS. The flexible resources on the demand side represented by internet data centers (IDCs) can realize the spatial-temporal migration of the load through the scheduling of the computation network. This can act as an active response resource to flexibly adjust the loads of the distribution network. In terms of spatial-temporal flexible resources, the deployment of large-scale IDCs has become an inevitable trend in the development of distribution networks because of the increasing requirements for computation and control. To increase the operational stability of CPDS, IDCs can flexibly adjust the spatial distribution of loads, thus reducing voltage becoming excessive [26], relieving network congestion [27], and shaving load peaks [28]. On operational economics, studies have been conducted to achieve the optimal comprehensive operating cost [29] and renewable energy consumption [30] of the power system through spatial scheduling of IDCs. Therefore, IDCs, as a type of spatial-temporal resource, have the potential to enhance the consumption capacity of distributed energy while reducing the operational costs.

This paper proposes an integrated planning method for distribution networks that addresses the bottleneck of cyber-physical network coordination and spatial-temporal flexible resource utilization. The main contributions are:

1) A cyber-physical integrated planning scheme is proposed. It takes into account the distributed control characteristics of ESSs and the spatial-temporal migration potential of data loads. This scheme enhances the economy of planning, promotes the access of DGs and optimizes overall resource allocation.

2) A three-layer optimization model is established. The upper, middle and lower layers are iteratively optimized to realize optimal allocation of physical resources (ESSs and smart terminal units (STUs)), spatial-temporal migration of data loads, and topology optimization of communication networks, respectively. The simulate anneal-particle swarm optimization (SA-PSO) algorithm is used to improve the solving accuracy and global optimization ability.

3) The convergence speed of distributed control is improved by optimizing the topology of on the cyber side. This enhancement significantly improves the controllability and practicability of the integrated planning scheme.

The remainder of this paper is structured as follows. Section II presents the general framework of CPDS and elaborates on the manner of the cyber-physical interac-

tion. Section III provides a detailed exposition of the modeling of spatial-temporal flexible resources (including ESSs and IDCs) and corresponding distributed control methods in CPDS. In Section IV, the integrated planning model of CPDS is proposed, along with the optimization algorithm and solving process. Section V verifies the economics and rationality of the proposed planning scheme using case studies, while Section VI presents the conclusion.

II. CPDS AND CROSS-LAYER NETWORK INTEGRATION

CPDS comprises three main networks: physical, communication and computation [31], [32], as illustrated in Fig. 1. As the number of coupling devices such as base stations, IDCs, and DGs increases in the CPDS system, the reliance on computation and communication networks for achieving cross-layer coupling of energy, information, and data flows becomes more pronounced. This contrasts with traditional centralized control devices, which do not have such extensive reliance on these networks.

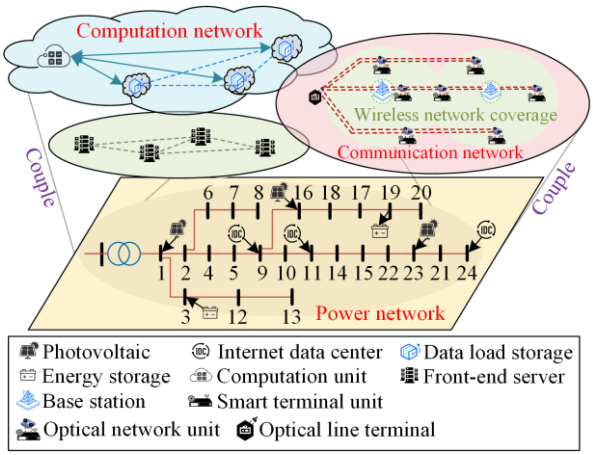

Fig. 1. Architecture of CPDS and cross-layer network integration.

1) Physical network. The physical network encompasses diverse physical devices, including power lines, distributed photovoltaics (PV), and ESS. These devices are perceived as monitored and controlled objects in CPDS, often requiring the installation of smart terminal units (STUs) to measure, collect, and analyze the operational data. As interfaces for flexible resource cross-network coupling, STUs facilitate centralized or distributed control over physical resources via the dispatching center. The real-time acquisition of measurement data from these physical devices by STUs is critical for enabling cyber-physical interactions within CPDS.

2) Communication network. The communication network comprises two main types: wired and wireless. The former consists of various components, including an optical line terminal (OLT), optical fibers, a passive optical splitter (POS), and an optical network unit (ONU) [20]. The last uses a mesh networking structure, in which the base station and its communication coverage serve as the foundation for wireless communication. Information flow is used to transmit data from each STU through the communication network. The communication network also enables flexible control of various active response resources and facilitates the transformation of control signals into executions.

3) Computation network. The computation network comprises IDCs, data load storage, and computation units. As a type of flexible resource, IDCs facilitate the flexible migration of data loads using a separate optical fiber network. Compared to electrical cables, optical fibers possess wider transmission bandwidth, lower transmission loss, and stronger anti-interference capability, thus providing a potential method for indirectly migrating power loads within the computation network, leading to substantial cost savings while enhancing operational reliability. This fosters effective interaction between data flows from the physical network and the computation network.

Within the CPDS network integration framework, distribution system planners can effectively comprehend the status of the network, ensure coordinated operation of multiple types of distributed resources, and monitor devices safely and in real time through the cyber system. This facilitates the full utilization of the active response potentials of distributed resources, enabling enhanced DG access and flexible resource regulation. Also, the investment costs associated with implementing a cyber device are significantly lower than those of a physical device (such as new lines or transformers). Thus, the relevant objectives of distribution network planning can be achieved in a more economically viable manner through reasonable communication equipment configuration while simultaneously improving system reliability.

III. SPATIAL-TEMPORAL FLEXIBLE RESOURCE MODELING IN CPDS

This section establishes the models of the physical and cyber resources present in CPDS, serving as a reference for subsequent planning scenarios. Mature modeling methods already exist for distributed PV systems, power lines, and other resources discussed in Section II, and thus the focus of this section is on the modeling of spatial-temporal flexible resources, delineating their involvement in integrated planning. The spatial-temporal flexibility resources considered in this paper encompass ESS and IDC.

A. ESS Model Considering Distributed Control

In normal circumstances, it is imperative to maintain the node voltage within a desirable range. However, if a high proportion of DG access results in the node voltages exceeding these limits, droop control can be applied to regulate the power absorbed or released by the ESSs, thereby stabilizing the voltages. In situations where a node voltage exceeds the upper limit of the normal voltage, the ESS operates in a charging state and absorbs a portion of the active power, thus mitigating

the voltage rise problem. Conversely, when a node voltage falls below the lower limit, the ESS discharges and releases active power to increase the node voltage. The active power of ESS during the droop control state can be expressed as [33], [34]:

$$P_n^{\text{droop}} = \begin{cases} \alpha(V_n - V_n^{\max}),\ V_n > V_n^{\max} \\ \beta(V_n - V_n^{\min}),\ V_n < V_n^{\min} \\ 0,\ V_n^{\min} < V_n < V_n^{\max} \end{cases} \tag{1}$$

where n is the number of nodes; V_n denotes the node voltage of n; $V_n^{\max}$ and $V_n^{\min}$ denote the upper and lower limits of the normal voltage, respectively. Equation (1) implies that larger values of exceeding voltage would result in the release or absorption of greater active power, thereby facilitating the mitigation of voltage excess. The droop coefficients α and β are determined by the maximum PV power $P_{\text{PV}}^{\max}$, maximum load power $P_{\text{L}}^{\max}$, and node rated voltage V_n^{rated} as:

$$\alpha = \frac{P_{\text{PV}}^{\max} - P_{\text{L}}^{\max}}{V_n^{\max} - V_n^{\text{rated}}} \tag{2}$$

$$\beta = \frac{P_{\text{PV}}^{\max} - P_{\text{L}}^{\max}}{V_n^{\text{rated}} - V_n^{\min}} \tag{3}$$

In addition, the active power of droop control P_n^{droop} can also be expressed by the ESS state of charge (SOC) variation, i.e.

$$P_n^{\text{droop}} = \frac{E_n \Delta SOC_{n,t}}{\Delta t} \tag{4}$$

where $\Delta SOC_{n,t}$ is the variation of SOC; E_n is the nth ESS's capacity; and Δt denotes the charging or discharging time.

Thus, the amount of SOC variation for each period for different ESSs can be expressed as follows:

$$\Delta SOC_{n,t} = \frac{P_n^{\text{droop}} \Delta t}{E_n} = \begin{cases} \dfrac{(P_{\text{PV}}^{\max} - P_{\text{L}}^{\max})(V_n - V_n^{\max})\Delta t}{(V_n^{\max} - V_n^{\text{rated}})E_n}, \\ V_n > V_n^{\max} \\ \dfrac{(P_{\text{PV}}^{\max} - P_{\text{L}}^{\max})(V_n - V_n^{\min})\Delta t}{(V_n^{\text{rated}} - V_n^{\min})E_n}, \\ V_n < V_n^{\min} \\ 0,\ V_n^{\min} < V_n < V_n^{\max} \end{cases} \tag{5}$$

This paper adopts distributed control to realize information transmission among different ESSs, catering for the practical construction of communication networks [35]. Distributed control allows for effective data interaction and information sharing between neighboring communication nodes via peer-to-peer communication, thus avoiding long-distance data transmission and communication congestion. Given the diversity of installed ESS capacity, SOC is usually used as a consistency variable to optimize the utilization of ESS. In ESS distributed control, in cases where the voltage limit is exceeded at a node, the immediate communication of voltage variation information is shared with other nodes via the communication network. Subsequently, each ESS applies appropriate regulation of the output based on the corresponding SOC, with the objective of restoring the voltage of the affected node to the normal range. For the whole distribution network, ESSs need to ensure enough power support to cope with the voltage excess problem. For an individual ESS, distributed control needs to achieve a uniform sharing of active power regulation to prevent some ESSs from consistently having high levels of active power regulation, which could deteriorate their operating life and operational effectiveness.

The performance of distributed control is closely linked to the topology of the communication network. Specifically, for any communication graph $\boldsymbol{g} = \{\boldsymbol{N}, \boldsymbol{\varepsilon}\}$, communication topology can be represented by a status transition matrix $\boldsymbol{A}$ in which the elements are directly related to the outdegree and indegree of the communication nodes. In cases where the communication network takes the form of a strongly connected graph, the elements A_{ij} in $\boldsymbol{A}$ can be mathematically expressed as [36]:

$$A_{ij} = \begin{cases} \dfrac{1}{1 + X_i^+},\ j = i \\ \dfrac{1}{1 + X_i^+},\ j \neq i,\ (i,j) \in \boldsymbol{\varepsilon} \\ 0,\ j \neq i,\ (i,j) \notin \boldsymbol{\varepsilon} \end{cases} \tag{6}$$

where $\boldsymbol{N}$ denotes the set of communication nodes, $i, j \in \boldsymbol{N}$; $\boldsymbol{\varepsilon}$ denotes the set of communication edges; $(i,j) \in \boldsymbol{\varepsilon}$ indicates that node i can communicate with node j; and X_i^+ denotes the indegree of node i. When SOC variation is used as the control variable, the SOC relationship between different nodes possessing communication connections can be mathematically characterized, provided that the communication topology adheres to a strongly connected graph [36], [37], as follows:

$$SOC_j[T+1] = \sum_{i \in \{\boldsymbol{N}_j^-\} \cup \{j\}} A_{ij} SOC_j[T] \tag{7}$$

where $\boldsymbol{N}_j^-$ indicates the set of neighbors of node j; $i \in \{\boldsymbol{N}_j^-\} \cup \{j\}$ indicates that i is the downstream node of j,i.e., nodes i can receive communication information from node j; and T is the number of iterations.

The convergence of distributed control is independent of the communication topology according to (6) and (7). However, the convergence speed directly correlates with the topology of the communication network, as the efficiency of information transmission and interaction hinges on the network structure [34], [35]. Therefore this paper emphasizes the significance of communication topology planning to optimize the effectiveness of the planning scheme during actual operation.

B. IDC Model Considering Data Load Spatial-temporal Migration

IDCs, as a type of crucial DR resource in the CPDS, can realize the spatial-temporal migration of data loads through the coupling of computation and power networks. However, since IDCs and power systems operate in different information environments, achieving mutual benefits can be challenging. This in turn poses difficulties for multiresource planning. This section first formulates a model for IDCs to illustrate the way data load processing occurs. Subsequently, the DR potential of IDCs is evaluated, and a model for spatial-temporal migration of data loads is developed. Figure 2 depicts a schematic diagram of the IDC coupling architecture and the spatial-temporal migration of data loads, whereas Fig. 3 illustrates their spatial-temporal migration [38].

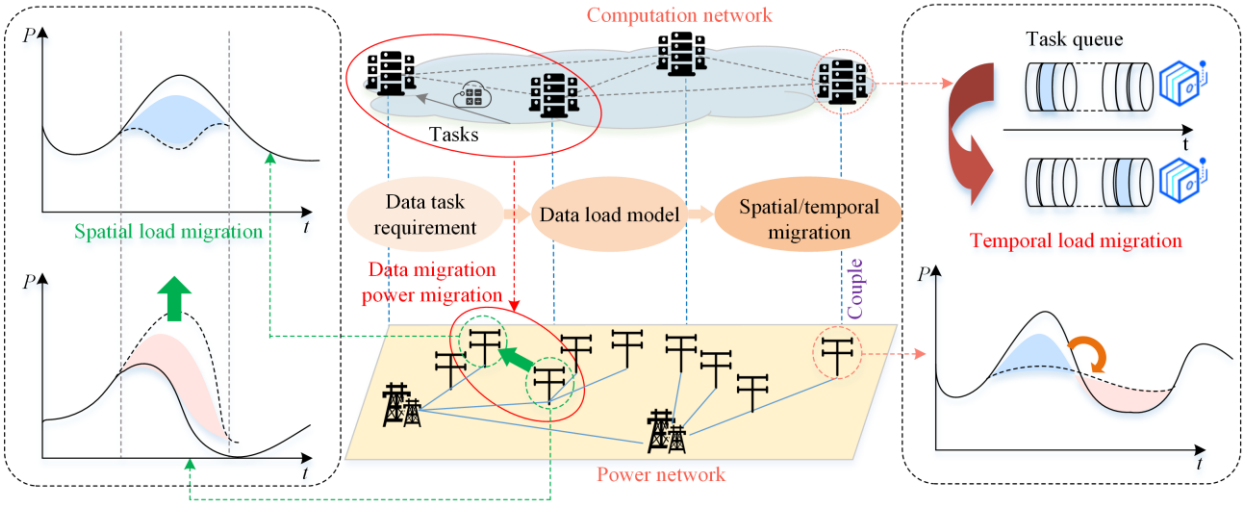

Fig. 2. IDC coupling architecture and data load spatial-temporal migration.

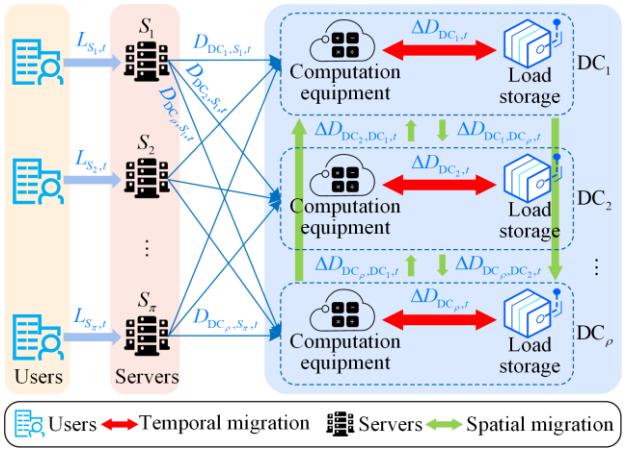

Fig. 3. Delay-tolerant data load spatial-temporal migration manner.

Within the context of CPDS, the data load processing procedure for IDCs can be distilled into three principal steps [39]:

1) Local users initiate task requests and upload the demand information to front-end servers through the computation network. This facilitates the formation of the data load model.

2) IDCs proceed to collect, analyze, and process the data load.

3) IDCs further distribute the data load migration among individual nodes, eventually resulting in the formulation of a computation node model.

The processing of data loads within CPDS is typically categorized into two distinct types: delay-sensitive and delay-tolerant [39]. The former necessitates real-time processing within a strict time limit, ensuring that all data loads received by individual IDCs are processed within this stipulated timeframe. The latter exhibits higher tolerances toward processing time and can be completed within specified intervals. This paper focuses on delay-tolerant data loads, and their spatial-temporal migration potential is used to realize their flexible operation. To ensure optimal performance, the data loads exchanged between front-end servers and computation nodes within IDCs must satisfy the following constraints [40]:

$$L_{S_k,t}=\sum_{r=1}^{\rho}D_{\mathrm{DC}_r,S_k,t}\ , \quad \forall t,\ k=1,2,\cdots,\pi;\ r=1,2,\cdots,\rho \tag{8}$$

$$D_{\mathrm{DC}_r,t}=\sum_{k=1}^{\pi}D_{\mathrm{DC}_r,S_k,t}+\sum_{\substack{r^*=1\\ r^*\neq r}}^{\rho}\Delta D_{\mathrm{DC}_r,\mathrm{DC}_{r^*},t}-\Delta D_{\mathrm{DC}_r,t}, \quad \forall t,\ k=1,2,\cdots,\ \pi,\ r=1,2,\cdots,\rho \tag{9}$$

where $L_{S_k,t}$ denotes the local user demand of the S_kth front-end server; k denotes the number of front-end servers; π denotes the total number of front-end servers; r denotes the number of IDCs; ρ denotes the number of computation nodes (IDCs); $D_{\mathrm{DC}_r,S_k,t}$ denotes the data load allocated to data center DC_r by the S_kth front-end server at time period t; $\Delta D_{\mathrm{DC}_r,\mathrm{DC}_{r^*},t}$ denotes the amount of data load migrated from DC_{r^*} to DC_r spa-

tially at time period t; while $D_{\mathrm{DC}_r,t}$ and $\Delta D_{\mathrm{DC}_r,t}$ denote the amount of data loads processed and temporally migrated to load storage by data center DC_r at time period t, respectively.

Equation (8) indicates that the sum of the data loads allocated by each front-end server regulation should equal the local user demand, while (9) indicates that the data loads to be processed at each IDC at each moment should equal the difference between the spatial migration data loads and the temporal migration loads.

Thus, the spatial-temporal flexible migration model for data loads can be mathematically formulated as follows:

$$\Delta D_{\mathrm{DC}_r,t}=\sum_{k=1}^{\pi}D_{\mathrm{DC}_r,S_k,t}+\sum_{\substack{r^*=1\\ r^*\neq r}}^{\rho}\Delta D_{\mathrm{DC}_r,\mathrm{DC}_{r^*},t}-D_{\mathrm{DC}_r,t} \tag{10}$$

$$\sum_{r=1}^{\rho}D_{\mathrm{DC}_r,t+1}=\sum_{r=1}^{\rho}D_{\mathrm{DC}_r,t}+\Delta D_{\mathrm{DC}_r,t}(\Delta t) \tag{11}$$

$$0\leqslant\sum_{r=1}^{\rho}D_{\mathrm{DC}_r,t}\leqslant D_{\max} \tag{12}$$

$$0\leqslant\sum_{\substack{r^*=1\\ r^*\neq r}}^{\rho}\Delta D_{\mathrm{DC}_r,\mathrm{DC}_{r^*},t}\leqslant D_{\mathrm{DC}_r,\max}\ \forall r,\ r\neq r^*,\ \forall t \tag{13}$$

$$\Delta D_{\mathrm{DC}_r,\mathrm{DC}_{r^*},t}\Delta D_{\mathrm{DC}_{r^*},\mathrm{DC}_r,t}\leqslant 0\ \forall r,\ \forall r^*,\ \forall t,\ r\neq r^* \tag{14}$$

where $D_{\max}$ denotes the upper limit of the total storage amount of the data loads in the data centers of CPDS and $D_{\mathrm{DC}_r,\max}$ denotes the upper limit of the data load spatial migration amount. Equations (10)–(12) consist of the data load temporal migration, and (13), (14) consist of the data load spatial migration.

IV. Cyber-Physical Integrated Planning Model and Optimization Algorithm

A. Optimization Model

Based on the flexible resource model established in Section III, this section proposes a three-layer optimization model to realize cyber-physical integrated planning. Considering the comprehensive utilization of the response potential of spatial-temporal flexible resources in CPDS, the optimal economy and reliability of the distribution network are realized. The control performance of the system is improved by optimizing the communication network topology. The hierarchical modeling design is as follows.

The upper layer focuses on the planning for ESSs and corresponding STUs. Its optimization variables include the optimal number and placement of ESSs and corresponding STUs, while minimizing equipment investment costs, ESS and IDC operation costs, loss costs, and optimizing distributed control performance. The middle layer caters to a data load flexible migration strategy based on the configuration of the upper layer, allowing for flexible spatial-temporal migration to minimize network loss and PV curtailment cost and enabling multiresource economic operation of CPDS. The lower layer is grounded in the upper layer planning scheme and the middle layer regulation strategy, with communication network topology optimization that solves the voltage excess problem in conjunction with distributed control performance. Given the above concept, the three-layer optimization model shown in Fig. 4 can be established, in which the solution is achieved by interrelating and iterating between the three layers. The model aims to comprehensively solve the voltage excess issue resulting from the incorporation of distributed energy sources within CPDS and improves the economy of the system by leveraging the spatial and temporal flexibility of resources. The convergence speed of distributed control is improved, and the flexibility of system operation is enhanced by optimizing the communication topology at the planning stage.

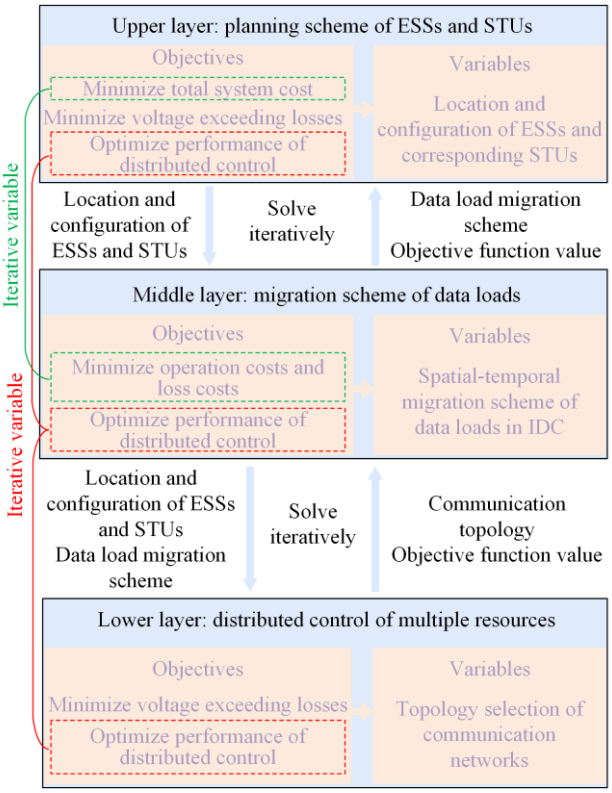

Fig. 4. Three-layer integrated planning model in CPDS.

B. Objective Function

1) Objective 1: Minimize Total System Cost

$$f_{\mathrm{CPDS}}^{\mathrm{inv}}=f_{\mathrm{ESS}}^{\mathrm{inv}}+f_{\mathrm{STU}}^{\mathrm{inv}}+f_{\mathrm{ESS}}^{\mathrm{op}}+f_{\mathrm{IDC}}^{\mathrm{op}}+f_{\mathrm{net}}^{\mathrm{loss}}+f_{\mathrm{PV}}^{\mathrm{loss}}+f_{\mathrm{EENS}}^{\mathrm{loss}} \tag{15}$$

a) Investment Cost

$$f_{\mathrm{ESS}}^{\mathrm{inv}}=\frac{d(1+d)^{y_1}}{(1+d)^{y_1}-1}\sum_{m=1}^{M}E_mC_{\mathrm{ESS}}^{\mathrm{inv}} \tag{16}$$

where $C_{\mathrm{ESS}}^{\mathrm{inv}}$ denotes the investment cost of the unit capacity of ESS; E_m is the mth ESS capacity; M de-

notes the number of planned ESSs; y_1 is the operating life of the ESSs (since the distributed control considers the uniform sharing of active power adjustment across ESSs, it is assumed that the operating life is the same across all ESSs); and d is the discount rate.

$$f_{\mathrm{STU}}^{\mathrm{inv}}=\frac{d(1+d)^{y_2}}{(1+d)^{y_2}-1}KC_{\mathrm{STU}}^{\mathrm{inv}} \tag{17}$$

where $C_{\mathrm{STU}}^{\mathrm{inv}}$ denotes the investment cost of a single STU; K is the planned number of STUs; and y_2 denotes the operating life of STUs.

This paper assumes that the number and configuration of IDCs have been determined. Therefore, only the spatial-temporal migration of their data loads is considered, without considering the investment costs of IDCs and corresponding servers.

b) Operational Cost

$$f_{\mathrm{ESS}}^{\mathrm{op}}=365\sum_{t=1}^{T}\sum_{m=1}^{M}C_{\mathrm{ESS}}^{\mathrm{unit}}\left|P_{\mathrm{ESS}}^{m,t}\right|\Delta T \tag{18}$$

where $C_{\mathrm{ESS}}^{\mathrm{unit}}$ denotes the operational and maintenance cost of the unit capacity of the ESS; $P_{\mathrm{ESS}}^{m,t}$ denotes the charging power or discharging power of the mth *ESS* during period t; T denotes the total number of charging and discharging time periods; and ΔT is the sampling interval. The operational cost for the ESS is converted into an equal annual cost.

$$f_{\mathrm{IDC}}^{\mathrm{op}}=365\sum_{t=1}^{T}\sum_{r=1}^{\rho}D_{r,t}MP_tP_{\mathrm{IDC}}^{t}\Delta T \tag{19}$$

where MP_t denotes the marginal price of the distribution network at time t (assuming the same price for each node in the distribution network); ρ is the number of IDCs; and P_{IDC}^{t} denotes the electrical energy needed by the IDCs to process a unit of data load per unit of time.

c) Loss Cost

$$f_{\mathrm{net}}^{\mathrm{loss}}=365\sum_{t=1}^{T}MP_tP_{\mathrm{loss}}^{t}\Delta T \tag{20}$$

where P_{loss}^{t} is the network loss in period t.

$$f_{\mathrm{PV}}^{\mathrm{loss}}=365\sum_{t=1}^{T}\sum_{n=1}^{N_k}MP_t(P_{\mathrm{PV}}^{n,t,\max}-P_{\mathrm{PV}}^{n,t})\Delta T \tag{21}$$

where $P_{\mathrm{PV}}^{n,t,\max}$ denotes the maximum active power consumption of the distributed PV at node n in period t; $P_{\mathrm{PV}}^{n,t}$ denotes the actual active power consumption; and N_k denotes the number of distributed PVs in the distribution network.

$$f_{\mathrm{EENS}}^{\mathrm{loss}}=365\sum_{t=1}^{T}\sum_{n=1}^{N}P_{\mathrm{EENS}}^{n,t}MP_t\Delta T \tag{22}$$

where $P_{\mathrm{EENS}}^{n,t}$ denotes the insufficient energy on the tth day of node n; and N denotes the number of physical nodes in the distribution network.

2) Objective 2: Minimize Voltage Excess Losses

By appropriately allocating ESSs and making full use of the flexible spatial and temporal scheduling characteristics of the data loads, the voltage excess problem can be mitigated, and the voltages can be maintained in a more stable fluctuation range. Our previous work has demonstrated that the allocation of ESSs and the migration of the data loads will inevitably reduce the consumption of distributed PV, resulting in a certain degree of curtailment and increased losses. However, the occurrence of transient voltage excess at individual nodes will not pose a danger and destructive loss to the system. Therefore, in this paper, the voltage fluctuation range is not considered as a constraint, whereas the node voltage excess losses are considered as an objective function for the optimal solution.

$$f_{\mathrm{voltage}}^{\mathrm{loss}}=\begin{cases}\xi\sum_{n=1}^{N}\sum_{\varphi\in\gamma}p_{\varphi}(V_n-V_n^{\max})\Delta T,\ V_n>V_n^{\max}\\ \xi\sum_{n=1}^{N}\sum_{\varphi\in\delta}p_{\varphi}(V_n^{\min}-V_n)\Delta T,\ V_n<V_n^{\min}\end{cases} \tag{23}$$

where φ is the set of voltage excess scenarios; p_{φ} denotes the probability of scenario φ; γ is the scenario set of voltage over the upper limit; δ is the scenario set of voltage below the upper limit; and ξ denotes the corresponding loss cost to unit voltage excess.

3) Objective 3: Optimal Performance of Distributed Control

The control performance of distributed control mainly considers its convergence speed, which is determined by the second largest eigenvalue of the status transition matrix $\boldsymbol{A}$ [36], [37]. A smaller second largest eigenvalue implies a faster convergence speed of distributed control. Therefore, the following performance indicator can be established to evaluate the convergence speed:

$$f_{\mathrm{con}}^{\mathrm{speed}}=\varphi(\boldsymbol{A}) \tag{24}$$

where $\varphi(\boldsymbol{A})$ denotes the numerical magnitude of the second largest eigenvalue of status transition matrix $\boldsymbol{A}$.

The objective functions and variables of each layer in the three-layer optimization model are shown in Fig. 4.

C. Constraints

1) Power Flow Constraints

The constraints of active and reactive power, node voltage and line current are presented respectively, as:

$$p_{j,t}=\sum_{i\in\sigma(j)}P_{ji,t}-\sum_{i\in\tau(j)}(P_{ij,t}-I_{ij,t}^2r_{ij})(t)+g_{ij}V_{j,t}^2,\ \forall j\in N,\ \forall t \tag{25}$$

$$q_{j,t}=\sum_{i\in\sigma(j)}Q_{ji,t}-\sum_{i\in\tau(j)}(Q_{ij,t}-I_{ij,t}^2x_{ij})(t)+b_{ij}V_{j,t}^2,\ \forall j\in N,\ \forall t \tag{26}$$

$$V_{j,t}^2 = V_{i,t}^2 - 2(P_{ij,t}r_{ij} + Q_{ij,t}x_{ij})(t) + I_{ij,t}^2(r_{ij}^2 + x_{ij}^2)(t), \quad \forall ij \in E,\ \forall t \tag{27}$$

$$I_{ij,t}^2 = \frac{P_{ij,t}^2 + Q_{ij,t}^2}{V_{i,t}^2},\ \forall ij \in E,\ \forall t \tag{28}$$

$$\begin{aligned} p_{j,t} &= P_{\mathrm{PV}}^{j,t} - P_{\mathrm{ESS}}^{j,t} - D_{j,t}P_{\mathrm{IDC}}^{t} - P_{\mathrm{load}}^{j,t} \\ q_{j,t} &= Q_{\mathrm{PV}}^{j,t} - Q_{\mathrm{ESS}}^{j,t} - Q_{\mathrm{load}}^{j,t} \end{aligned} \tag{29}$$

$$\left\| \begin{bmatrix} 2P_{ij,t} \\ 2Q_{ij,t} \\ I_{ij,t} - U_{i,t} \end{bmatrix} \right\|_2 \leqslant I_{ij,t} + U_{i,t} \tag{30}$$

where r_{ij} and x_{ij} are the respective values of the resistance and reactance of branch ij; while g_{ij} and b_{ij} are the values of conductance and reactance of branch ij, respectively; $p_{j,t}$ and $q_{j,t}$ represent the injected active and reactive power of node *j*, respectively; $I_{ij,t}$ and $U_{i,t}$ denote the branch current and node voltage, respectively; $P_{ij,t}$ and $Q_{ij,t}$ represent the active power and reactive power on line ij at period *t*, which are positive when flowing from node *i* to node *j*, while $i \in \sigma(j)$ and $i \in \tau(j)$ indicate that node *i* is the out-neighbor and in-neighbor of node *j*; respectively. Equation (29) represents the components of the injected active and reactive power, where $P_{\mathrm{PV}}^{j,t}$ and $Q_{\mathrm{PV}}^{j,t}$ denote the injected active and reactive power of distributed photovoltaic; $P_{\mathrm{ESS}}^{j,t}$ and $Q_{\mathrm{ESS}}^{j,t}$ denote the charging power of ESS; $P_{\mathrm{load}}^{j,t}$ and $Q_{\mathrm{load}}^{j,t}$ denote the load power.

Since (27) and (28) contain quadratic terms, their linear transformation is needed. The power flow constraint model based on the second-order cone programming (SOCP) is:

$$\begin{aligned} & P_{ij,t}^2 + Q_{ij,t}^2 \leqslant I_{ij,t}^2 V_{i,t}^2 \\ \Leftrightarrow\ & P_{ij,t}^2 + Q_{ij,t}^2 \leqslant \frac{(I_{ij,t}^2 + V_{i,t}^2)^2 - (I_{ij,t}^2 - V_{i,t}^2)^2}{4} \\ \Leftrightarrow\ & (2P_{ij,t})^2 + (2Q_{ij,t})^2 + (I_{ij,t}^2 - V_{i,t}^2)^2 \leqslant (I_{ij,t}^2 + V_{i,t}^2)^2 \\ \Leftrightarrow\ & \left\| \begin{matrix} 2P_{ij,t} \\ 2Q_{ij,t} \\ I_{ij,t}^2 - V_{i,t}^2 \end{matrix} \right\|_2 \leqslant I_{ij,t}^2 + V_{i,t}^2 \end{aligned} \tag{31}$$

2) Security Constraints

$$\underline{I_{ij,t}} \leqslant I_{ij,t} \leqslant \overline{I_{ij,t}},\ \forall ij \in E \tag{32}$$

$$p_{j,t}^{\min} \leqslant p_{j,t} \leqslant p_{j,t}^{\max} \quad \forall j \in N \tag{33}$$

$$q_{j,t}^{\min} \leqslant q_{j,t} \leqslant q_{j,t}^{\max} \quad \forall j \in N \tag{34}$$

where $\underline{I_{ij,t}}$ and $\overline{I_{ij,t}}$ are the lower and upper limits of the branch currents, respectively; $p_{j,t}^{\max}$ and $p_{j,t}^{\min}$ are the upper and lower active power limits of the nodes, respectively; while $q_{j,t}^{\max}$ and $q_{j,t}^{\min}$ are the upper and lower limits of nodal reactive power, respectively.

3) IDC Constraints

The IDC constraints are shown in (10)–(14).

4) ESS Constraints

ESS constraints are shown in (5)–(7). In addition, the following constraints need to be satisfied.

$$\underline{SOC}_j \leqslant SOC_j \leqslant \overline{SOC_j},\ \forall j \in \boldsymbol{N} \tag{35}$$

$$E_m^{\min} \leqslant E_m^t \leqslant E_m^{\max} \tag{36}$$

$$E_m^{t+\Delta t} = E_m^t + P_{m,t}^{\mathrm{ch}}\gamma_m^{\mathrm{ch}}\Delta t - \frac{P_{m,t}^{\mathrm{dis}}\Delta t}{\gamma_m^{\mathrm{dis}}} \tag{37}$$

where $\underline{SOC}_j$ and $\overline{SOC_j}$ are the lower and upper limits of the SOC, respectively; while $E_m^{\min}$ and $E_m^{\max}$ are the lower and upper limits of the ESS capacity, respectively; γ_m^{ch} and γ_m^{dis} denote the respective charging and discharging efficiencies of ESS; while $P_{m,t}^{\mathrm{ch}}$ and $P_{m,t}^{\mathrm{ch}}$ denote the charging and discharging power of the *m*th *ESS* during period *t*, respectively.

D. Optimization Algorithm and Solving Process

For multi-layer optimization models, the particle swarm optimization (PSO) algorithm has been a popular choice for tackling topology optimization and equipment location selection issues [41]. Nevertheless, when dealing with the iterative structure of the three-layer optimization model depicted in Fig. 4, the adoption of the PSO algorithm may result in local optimization because of the presence of numerous optimization dimensions within the model. Consequently, this paper employs the simulate anneal-particle swarm optimization (SA-PSO) algorithm, which represents an upgraded variant of the PSO algorithm. It comes with several noteworthy advantages compared to its precursor, e.g., enhanced global optimization capability, improved convergence speed, parameter setting flexibility and superior performance in high-dimensional problems.

The upper optimization variables in the proposed model are the locations and capacities of the ESSs and corresponding STUs, the middle optimization variable is the data load spatial-temporal flexibility regulation strategy, and the lower optimization variable is the communication network topology. The flow chart of the optimization algorithm is detailed in Fig. 5.

From the optimization algorithm in Fig. 5, the iterative solving process of the proposed three-layer optimization model can be performed. The upper layer's output permeates the middle layer, resulting in further refinement of the data load flexible migration strategy. The middle layer's outcomes then steer the optimization process for communication network topology in the

lower layer, which subsequently feeds back to the upper layer with improved planning insights. This iterative cycle operates until convergence is achieved, culminating in an optimal solution that takes into consideration all three layers' objectives. It is worth mentioning that the introduction of a middle layer in the optimization model enables more sophisticated optimizations compared to the incorporation of the IDC data load migration scheme in the upper-level model. This enhancement leads to the production of a superior solution and an overall improvement in efficiency and solving process.

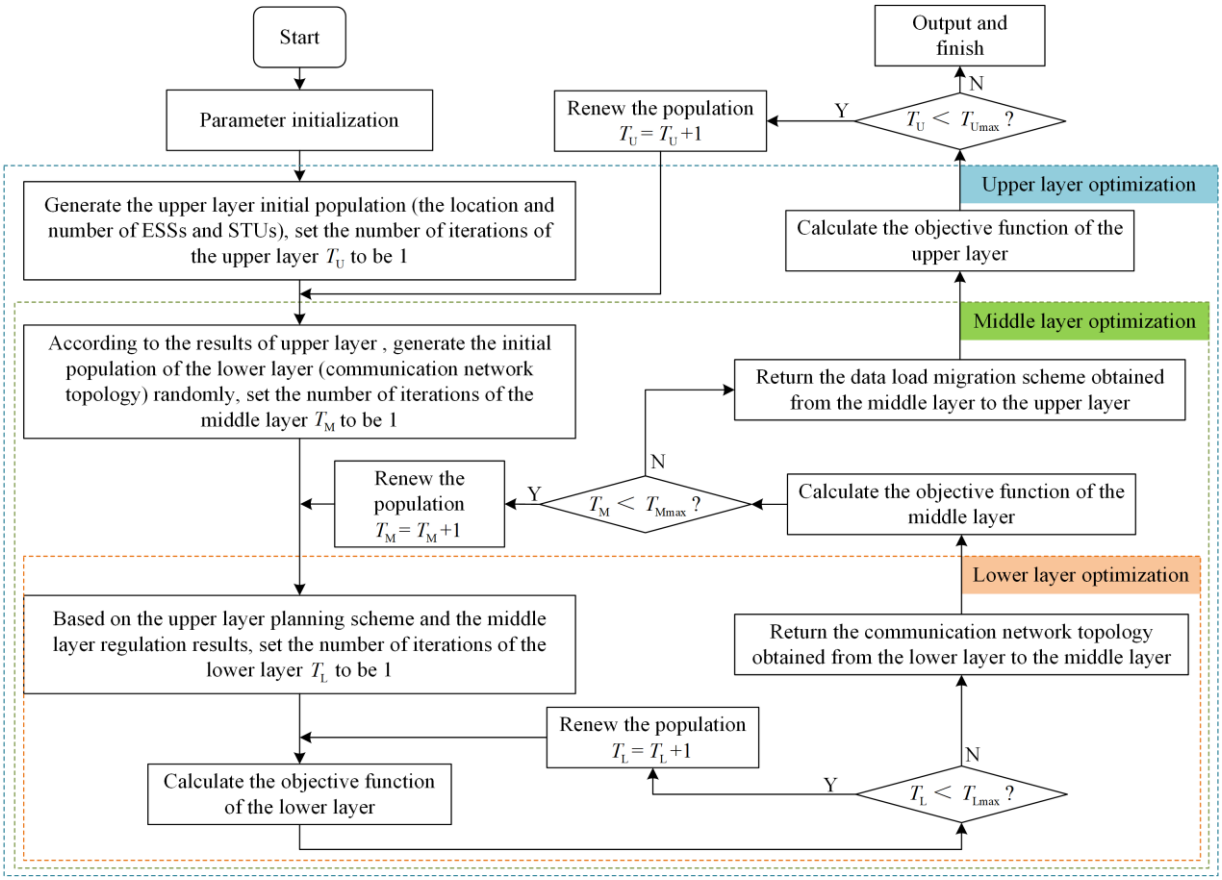

Fig. 5. Flow chart of the proposed optimization algorithm.

V. Case Study

A. Case Settings

This section uses the modified IEEE 33-bus distribution network to verify the practical effect of the above integrated planning scheme. The system model is shown in Fig. 6. The rated voltage is 12.66 kV, and the total active and reactive power demand of the network are 3715 kW and 2300 kvar, respectively.

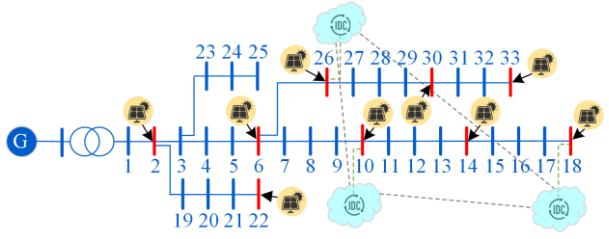

Fig. 6. Modified IEEE 33-bus distribution system.

The marked buses in Fig. 6 are distributed PV access nodes as well as ESS planning locations to be selected. The PV rated output is 600 kW, and typical daily PV output and electric load power curves are shown in Fig. 7.

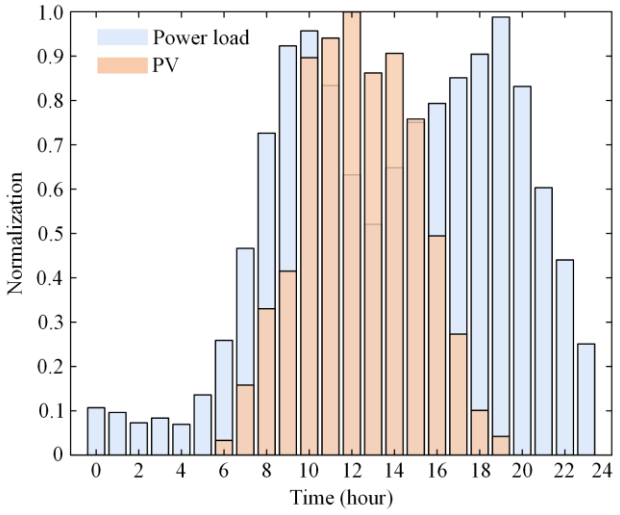

Fig. 7. Typical PV output and power load curve.

The load power factor is 0.95, and the maximum installed capacity of the ESS is 200 kWh. Three data centers are installed at nodes 10, 18 and 26, respectively. The typical daily data load curves of the data centers and the time-of-use (TOU) price are shown in Fig. 8. The data loads of different data centers can be spatially migrated, and the data loads within each data center can be temporally migrated, in addition to not accounting for other energy consumption within the data center.

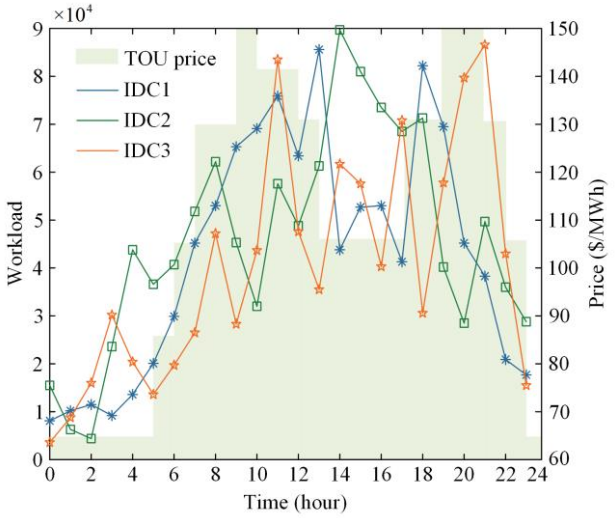

Fig. 8. Typical daily data load and TOU curve.

Other parameters in the planning model are set as shown in Table I.

TABLE I
PARAMETER SETTINGS

Parameter settings	Value
Investment cost per unit capacity of ESS $C_{\mathrm{ESS}}^{\mathrm{inv}}$ (¥/kWh)	0.25×10^4
Investment cost of a single STU $C_{\mathrm{STU}}^{\mathrm{inv}}$ (¥)	0.20×10^4
Operational life of ESS y_1 (years)	10
Operational life of STU y_2 (years)	10
Discount rate d (%)	8
Unit capacity ESS operation cost $C_{\mathrm{ESS}}^{\mathrm{unit}}$ (¥/kW)	0.20×10^4
Lower limit of normal voltage $V_n^{\min}$ (p.u.)	0.95
Upper limit of normal voltage $V_n^{\max}$ (p.u.)	1.05
Upper limit of data loads storage in IDCs $Data_{\max}$	1.2×10^5
Power required to process a unit data load P_{IDC}^t (kW)	0.02

In this case, economy is the primary indicator of the multi-objective optimization problem, so the equipment investment cost is more important than the other two objectives. The distributed control performance is the second most important indicator to be considered. Minimizing the loss cost of voltage excess is related to the probability of voltage excess scenarios, and its influence in the optimization function can be weakened appropriately. The hierarchical analysis method is used to determine the weights of the three objective functions in the upper layer of the planning model in Fig. 4, and the judgment matrix in this case is set as follows:

$$\boldsymbol{\omega}=\begin{bmatrix}1 & 4 & 2\\ 1/4 & 1 & 1/2\\ 1/2 & 2 & 1\end{bmatrix} \tag{38}$$

B. Results and Analysis

The above distribution network model is optimally solved using the method in Section IV. The results of ESS location and capacity planning on the physical side are shown in Table II, and the corresponding costs of the planning scheme are shown in Table III. The results of communication network topology planning on the cyber side are shown in Fig. 9, while the voltage variation curve of each node in the planning scenario is shown in Fig. 10.

TABLE II
ESS LOCATION AND CONFIGURATION

Node Number	Node Number
2	150
10	100
14	150
18	100
26	200
Total	700

TABLE III
ANNUAL COST OF PLANNING SCHEME

Type of costs	Value (¥)
ESS investments	2.6082×10^6
STU investments	1.4903×10^6
ESS operation	3.3640×10^5
IDC operations	2.1470×10^6
Network losses	1.6090×10^5
PV curtailment losses	2.1410×10^5
EENS losses	8.3700×10^4
Annual cost	7.0406×10^6

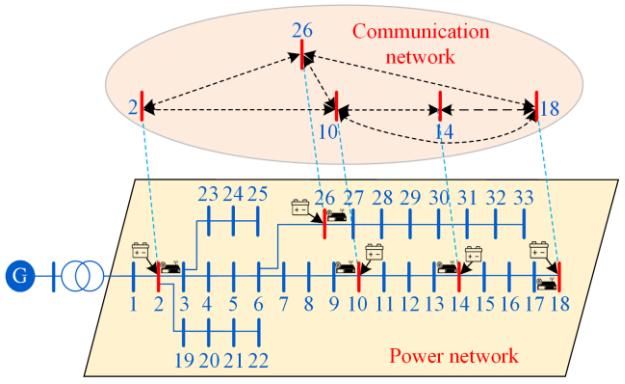

Fig. 9. Communications network topology planning results.

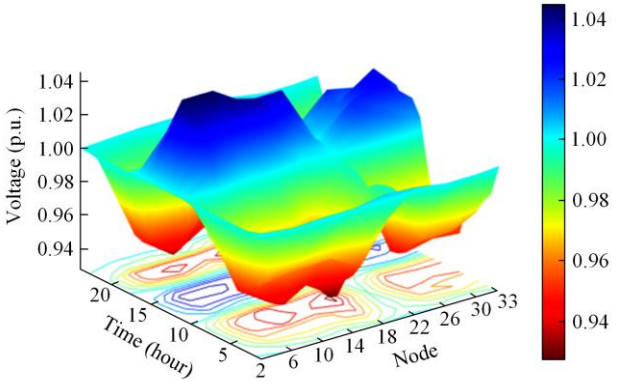

Fig. 10. Voltage variation curve of different nodes.

For the optimization problem proposed in this paper, the fitness function curve is shown in Fig. 11 (the PSO and SA-PSO algorithms are adopted). It demonstrates that the SA-PSO algorithm reaches convergence in only approximately 70 iterations, whereas the PSO algorithm requires approximately 110 iterations. The results obtained by the SA-PSO algorithm clearly outperform those of the PSO algorithm.

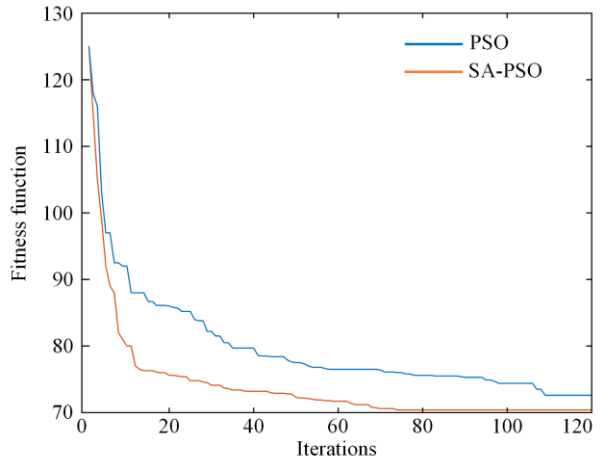

Fig. 11. Fitness function convergence curves (the PSO algorithm and SA-PSO algorithm are adopted).

C. Comparison of Different Schemes

To verify the economy and reliability of the proposed planning model, in this section three sets of comparisons are performed to compare the planning results before and after considering data load spatial-temporal migration, cyber-physical integrated planning, and voltage excess constraints.

1) Comparison of Schemes Before and After Considering Spatial-temporal Resources

Scheme 1: Traditional planning scheme (without spatial-temporal resources).

Scheme 2: Proposed planning scheme in this paper.

The ESS capacity configuration and annual costs of the above planning schemes are shown in Tables IV and V, respectively. As shown, after considering data load flexible migration, the data loads can be spatially shifted to computation nodes with lower loads and higher voltage values and can be temporally shifted to time periods with lower TOU prices. This migration approach offers two significant benefits: 1) active spatial scheduling of the data loads can balance the loads and thus reduce the demand for ESS capacity in the planning stage, resulting in reduced investment and operational costs; and 2) the flexible migration of data loads in time reduces the cost of purchasing power when the data center is running. It effectively reduces the amount of data load processing during peak electricity consumption, leading to a reduction in overall costs.

However, data load migration can also result in the reduction of PV consumption, which increases PV curtailment costs. Additionally, network loss and EENS loss will increase. Similarly, the overall analysis indicates that Scheme 2 results in an annual cost reduction of ¥ 1 752 700 when compared to Scheme 1. This outcome strongly suggests that considering data load migration is an effective way to improve the economy of the planning scheme.

TABLE IV
ESS PLANNING RESULTS BEFORE AND AFTER CONSIDERING THE SPATIAL-TEMPORAL MIGRATION OF DATA LOADS

Node	ESS capacity configuration (kWh)									
	2	6	10	14	18	22	26	30	33	Total
Scheme 1	100	100	50	100	150	0	200	0	150	850
Scheme 2	150	0	100	150	100	0	200	0	0	700

TABLE V
ANNUAL COSTS BEFORE AND AFTER CONSIDERING THE SPATIAL-TEMPORAL MIGRATION OF DATA LOADS

Schemes	ESS Investments (¥)	STU Investments (¥)	ESS operation costs (¥)	IDC operation costs (¥)	Network losses (¥)	PV curtailment losses (¥)	EENS losses (¥)	Annual costs (¥)
1	3.1671×10^6	2.0864×10^6	4.0030×10^5	2.8860×10^6	8.2500×10^4	1.0380×10^5	6.7200×10^4	8.7933×10^6
2	2.6082×10^6	1.4903×10^6	3.3640×10^5	2.1470×10^6	1.6090×10^5	2.1410×10^5	8.3700×10^4	7.0406×10^6

2) Comparison of Schemes Before and After Considering Cyber-physical Integration

Scheme 1: Traditional planning scheme (independent planning of the physical system and cyber system).

Scheme 2: Proposed planning scheme in this paper.

The ESS capacity configuration and annual costs of the above planning schemes are shown in Tables VI and VII, respectively. Table VII provides clear evidence that the integrated planning approach exhibits superior economy to that of the cyber-physical independent planning approach. The primary reason behind this is that the proposed method integrates ESSs and STUs for a more centralized configuration, thereby reducing communication investment in comparison to the decentralized approach. However, the decentralized configuration of ESSs allows for power balancing on-site, enhances PV consumption, and mitigates customer losses resulting from network loss and congestion. In terms of the annual cost, the integrated planning model presented in this study boasts specific advantages over independent planning models.

TABLE VI
ESS PLANNING RESULTS BEFORE AND AFTER CONSIDERING CYBER-PHYSICAL INTEGRATED PLANNING

Node	ESS capacity configuration (kWh)									
	2	6	10	14	18	22	26	30	33	Total
Scheme 1	100	100	50	100	150	50	200	50	100	900
Scheme 2	150	0	100	150	100	0	200	0	0	700

TABLE VII
ANNUAL COSTS BEFORE AND AFTER CONSIDERATION OF CYBER-PHYSICAL INTEGRATED PLANNING

Schemes	ESS Investments (¥)	STU Investments (¥)	ESS operation costs (¥)	IDC operation costs (¥)	Network losses (¥)	PV curtailment losses (¥)	EENS losses (¥)	Annual costs (¥)
1	3.3534×10^6	2.6825×10^6	4.5920×10^5	2.1846×10^6	6.3200×10^4	9.8700×10^4	5.3000×10^4	8.8946×10^6
2	2.6082×10^6	1.4903×10^6	3.3640×10^5	2.1470×10^6	1.6090×10^5	2.1410×10^5	8.3700×10^4	7.0406×10^6

3) Comparison of Schemes Before and After the Voltage Range is Strictly Restricted

Scheme 1: Use the voltage range as a constraint to strictly limit voltage excess.

Scheme 2: Proposed planning scheme in this paper, in which the voltage excess is used as the objective function.

Figures 12 and 13 illustrate the voltage variations of each node corresponding to the two schemes mentioned above. The annual costs of the above planning schemes are shown in Table VIII. According to Figs. 12 and 13 and Table VIII, strictly limiting the voltage excess through voltage range constraints leads to increased investment and operational costs. This constraint results in a significant reduction in data load temporal migration in order to prevent undervoltage at nodes under heavy loads, as well as reduced amount of data load spatial migration between IDCs, ultimately increasing data center operational costs. Additionally, if PV consumption is limited when the voltage exceeds its limit, a certain curtailment loss occurs. However, controlling the node voltage within a safe range reduces line loss and EENS loss, precluding voltage excess loss. Generally, the use of the integrated planning scheme proposed in this study can improve system economy and reliability, particularly when the planning scheme relaxes the voltage range constraint.

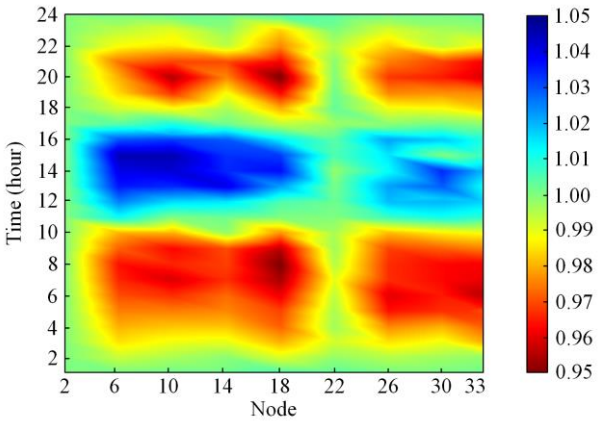

Fig. 12 Node voltage variation heatmap in Scheme 1.

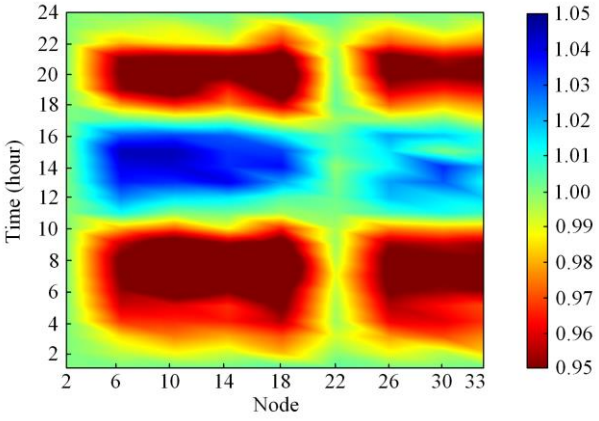

Fig. 13 Node voltage variation heatmap in Scheme 2.

TABLE VIII
ANNUAL COSTS BEFORE AND AFTER STRICTLY CONSTRAINED VOLTAGE RANGES

Schemes	ESS investments (¥)	STU investments (¥)	ESS operation costs (¥)	IDC operation costs (¥)	Network losses (¥)	PV curtailment losses (¥)	EENS losses (¥)	Voltage exceeding losses (¥)	Annual costs (¥)
1	2.7448×10^6	1.5862×10^6	3.6060×10^5	2.5095×10^6	1.1840×10^5	3.8920×10^5	4.4900×10^4	0	7.7536×10^6
2	2.6082×10^6	1.4903×10^6	3.3640×10^5	2.1470×10^6	1.6090×10^5	2.1410×10^5	8.3700×10^4	5.8300×10^4	7.0989×10^6

VI. SUMMARY

This paper has introduced an integrated planning model of CPDS with spatial-temporal flexible resources, and established a three-layer planning model to iteratively solve the planning problem. The following conclusions can be drawn:

1) The cyber-physical integrated planning scheme proposed in this paper can effectively allocate multiple types of distributed resources, resulting in reduced equipment investment costs. System reliability is improved by considering more operational constraints during the planning stage.

2) Data loads, as spatial-temporal flexible resources, can be migrated spatially to lower-load, higher-voltage computation nodes and temporally to periods with lower TOU prices, resulting in additional cost savings in power purchase costs.

3) The communication topology significantly influences the planning scheme as it determines the convergence speed of distributed control. Optimizing the communication network topology improves the overall distributed control performance of the system.

4) The case studies verify the economic advantages of the proposed scheme over the traditional method. The proposed scheme successfully mitigates voltage excess problems, providing an effective solution to the challenges encountered in CPDS planning.

ACKNOWLEDGMENT

Not applicable.

AUTHORS' CONTRIBUTIONS

Shutan Wu: methodology, data curation, formal analysis, investigation, resources, and original-draft writing. Qi Wang: conceptualization, methodology, funding acquisition, project administration, supervision, review-writing & editing. Qichao Chen: software, validation, and review-writing & editing. Changping Yu: visualization and original-draft writing. Yi Tang: supervision, review-writing & editing. All authors read and approved the final manuscript.

FUNDING

This work is supported by National Key R&D Program of China (No. 2019YFE0118000).

AVAILABILITY OF DATA AND MATERIALS

Please contact the corresponding author for data material request.

DECLARATIONS

The authors declare that they have no known competing financial interests or personal relationships that could have appeared to influence the work reported in this paper.

AUTHORS' INFORMATION

Shutan Wu received the B.E. degree and M.E. degree in electrical engineering from Southeast University, Nanjing, China, in 2021 and 2024, respectively, where he is currently pursuing the Ph.D. degree. His research areas include distribution system planning and operation control, and cyber-physical distribution system.

Qi Wang received the B.E., M.E., and Ph.D. degrees in electrical engineering from Southeast University, Nanjing, China, in 2011, 2013, and 2017, respectively. In 2014 and 2015, he conducted research with Virginia Polytechnic Institute and State University as a joint-training doctor. After his Ph.D. graduation, he joined Southeast University, where he is currently an Associate Professor. His research areas include power system stability analysis, and control, and cyber-physical power system.

Qichao Chen received the Ph.D. degree from the Harbin Institute of Technology, Harbin, China, in 2015. Since 2016, he has been an engineer with the State Grid Economic and Technological Research Institute CO,.LTD., Beijing, China. His research interests include power-electronics-based power system stability analysis and control.

Changping Yu is currently pursuing the M.E. degree in electrical engineering at Southeast University. Her research direction is flexible scheduling of distributed resources.

Yi Tang received the B.E., M.E., and Ph.D. degrees from the Harbin Institute of Technology, China, in 2000, 2002, and 2006, respectively. Since 2006, he has been working with the School of Electrical Engineering,

Southeast University, Nanjing, China. He is currently a Professor with Southeast University and the director of Power System Automation Research Institute. His research interests include smart grid, power system security, power system stability analysis, renewable energy systems, and cyber-physical systems.

REFERENCES

[1] R. A. Walling, R. Saint, and R. C. Dugan *et al*., "Summary of distributed resources impact on power delivery systems," *IEEE Transactions on Power Delivery*, vol. 23, no. 3, pp.1636-1644, Aug. 2008.

[2] K. Zou, A. P. Agalgaonkar, and K. M. Muttaqi *et al*., "Distribution system planning with incorporating DG reactive capability and system uncertainties," *IEEE Transactions on Sustainable Energy*, vol. 3, no. 1, pp. 112-123, Jan. 2012.

[3] D. Zhang, J. Li, and D. Hui, "Coordinated control for voltage regulation of distribution network voltage regulation by distributed energy storage systems," *Protection and Control of Modern Power Systems*, vol. 3, no. 1, pp. 1-8, Jan. 2018.

[4] H. S. Salama, G. Magdy, and A. Bakeer *et al*., "Adaptive coordination control strategy of renewable energy sources, hydrogen production unit, and fuel cell for frequency regulation of a hybrid distributed power system," *Protection and Control of Modern Power Systems*, vol. 7, no. 3, pp. 1-18, Jul. 2022.

[5] W. Liu, H. Xu, and Y. Chen *et al*., "Cyber physical distribution system optimal planning considering the influence of multidimensional uncertainties," *Proceedings of the CSEE*, vol. 37, no. 24, pp. 7205-7215, Dec. 2017. (in Chinese)

[6] H. Gao, X. Lyu, and S. He *et al*., "Integrated planning of cyber-physical active distribution system considering multidimensional uncertainties," *IEEE Transactions on Smart Grid*, vol. 13, no. 4, pp. 3145-3159, Jul. 2022.

[7] S. Kansal, V. Kumar, and B. Tyagi, "Optimal placement of different type of DG sources in distribution networks," *International Journal of Electrical Power & Energy Systems*, vol. 53, pp. 752-760, Dec. 2013.

[8] U. Sultana, A. B. Khairuddin, and M. M. Aman *et al.*, "A review of optimum DG placement based on minimization of power losses and voltage stability enhancement of distribution system," *Renewable and Sustainable Energy Reviews*, vol. 63, pp. 363-378, Sept. 2016.

[9] H. Falaghi, C. Singh, and M. R. Haghifam *et al*., "DG integrated multistage distribution system expansion planning," *International Journal of Electrical Power & Energy Systems*, vol. 33, no.8, pp. 1489-1497, Oct. 2011.

[10] J. H. Yi, R. Cherkaoui, and M. Paolone *et al*., "Expansion planning of active distribution networks achieving their dispatchability via energy storage systems," *Applied Energy*, vol. 326, Nov. 2022.

[11] J. Y. Park, J. M. Sohn, and J. K. Park, "Optimal capacitor allocation in a distribution system considering operation costs," *IEEE Transactions on Power Systems*, vol. 24, no. 1, pp. 462-468, Feb. 2009.

[12] P. Li, J. Ji, and S. Che *et al*., "Multi-stage expansion planning of energy storage integrated soft open points considering tie-line reconstruction," *Protection and Control of Modern Power Systems*, vol.7, no. 4, pp. 1-15, Oct. 2022.

[13] B. Stojanović, T. Rajić, and D. Šošić, "Distribution network reconfiguration and reactive power compensation using a hybrid simulated annealing-minimum spanning tree algorithm," *International Journal of Electrical Power & Energy Systems*, vol. 147, May 2023.

[14] H. Gao and J. Liu, "Coordinated planning considering different types of DG and load in active distribution network," *Proceedings of the CSEE*, vol. 36, no. 18, pp. 4911-4918, Sept. 2016.(in Chinese)

[15] J. Xiao, Z. Zhang, and L. Bai *et al*., "Determination of the optimal installation site and capacity of battery energy storage system in distribution network integrated with distributed generation," *IET Generation, Transmission & Distribution*, vol. 10, no. 3, pp. 601-607, Feb. 2016.

[16] H. Zhong, G. Zhang, and Z. Tan *et al*. "Hierarchical collaborative expansion planning for transmission and distribution networks considering transmission cost allocation," *Applied Energy*, vol. 307, Feb. 2022.

[17] H. Gao, J. Liu, and Z. Wei *et al*., "A bi-level robust planning model of active distribution network and its solution method," *Proceedings of the CSEE*, vol. 37, no. 5, pp. 1389-1400, Mar. 2017. (in Chinese)

[18] S. Dehghan, N. Amjady, and A. Kazemi, "Two-stage robust generation expansion planning: a mixed integer linear programming model," *IEEE Transactions on Power Systems*, vol. 29, no. 2, pp. 584-597, Mar. 2014.

[19] J. F. Franco, M. J. Rider, and R. Romero, "A mixed-integer quadratically-constrained programming model for the distribution system expansion planning," *International Journal of Electrical Power & Energy Systems*, vol. 62, pp. 265-272, Nov. 2014.

[20] X. Lyu, H. Gao, and S. He *et al*., "Integrated planning of cyber-physical active distribution system considering hybrid communication networking," *Proceedings of the CSEE*, vol. 43, no. 13, pp. 4987-5001, Jul. 2022. (in Chinese)

[21] F. Ahsan, N. H. Dana, and S. K. Sarker *et al*., "Data-driven next-generation smart grid towards sustainable energy evolution: techniques and technology review," *Protection and Control of Modern Power Systems*, vol. 8, no. 3, Jul. 2023.

[22] M. Song, Y. Cai, and C. Gao *et al*., "Transactive energy in power distribution systems: Paving the path toward cyber-physical-social system", *International Journal of Electrical Power & Energy Systems*, vol. 142, Nov. 2022.

[23] W. Liu, Q. Gong, and H. Han *et al*., "Reliability modeling and evaluation of active cyber physical distribution system," *IEEE Transactions on Power Systems*, vol. 33, no. 6, pp. 7096-7108, Nov. 2018.

[24] C. Chen, C. Lin, and H. Chuang *et al*., "Optimal placement of line switches for distribution automation systems using immune algorithm," *IEEE Transactions on Power Systems*, vol. 21, no. 3, pp. 1209-1217, Aug. 2006.

[25] J. Liu, H. Cheng, and Z. Zhang, "Planning of terminal unit amount in distribution automation systems," *Automation of Electric Power Systems*, vol. 37, no.12, pp. 44-50, May 2013. (in Chinese)

[26] S. Chen, P. Li, and H. Ji *et al*., "Operational flexibility of active distribution networks with the potential from data centers," *Applied Energy*, vol. 293, Jul. 2021.

[27] M. Chen, C. Gao, and M. Shahidehpour *et al*., "Incentive-compatible demand response for spatially coupled internet data centers in electricity markets," *IEEE Transactions on Smart Grid*, vol. 12, no. 4, pp. 3056-3069, Jul. 2021.

[28] C. Guo, F. Luo, and Z. Cai *et al.*, "Integrated planning of internet data centers and battery energy storage systems in smart grids," *Applied Energy*, vol. 281, Jan. 2021.

[29] S. Wu, Q. Wang, and B. Chen, "Collaborative planning of cyber physical distribution system considering the flexibility of data centers", *Energy Reports*, vol. 9, pp. 656-664, Sept. 2023.

[30] T. Yang, H. Jiang, and Y. Hou *et al*., "Study on carbon neutrality regulation method of interconnected multi-datacenter based on spatio-temporal dual-dimensional computing load migration," *Proceedings of the CSEE*, vol.42, no.1, pp.164-177, Jan. 2022. (in Chinese)

[31] H. Wang, Q. Wang, and Y. Tang *et al*., "Spatial load migration in a power system: concept, potential and prospects," *International Journal of Electrical Power & Energy Systems*, vol. 140, Sept. 2022.

[32] L. Parolini, B. Sinopoli, and B. H. Krogh *et al.*, "A cyber-physical systems approach to data center modeling and control for energy efficiency," *Proceedings of the IEEE*, vol. 100, no. 1, pp. 254-268, Jan. 2012.

[33] L. Xing, Y. Mishra, and Y. Tian *et al*., "Distributed voltage regulation for low-voltage and high-PV-penetration networks with battery energy storage systems subject to communication delay," *IEEE Transactions on Control Systems Technology*, vol. 30, no. 1, pp. 426-433, Jan. 2022.

[34] Y. Wang, K. T. Tan, and X. Y. Peng *et al*., "Coordinated control of distributed energy-storage systems for voltage regulation in distribution networks," *IEEE Transactions on Power Delivery*, vol. 31, no. 3, pp. 1132-1141, Jun. 2016.

[35] M. Zeraati, M. E. Hamedani Golshan, and J. M. Guerrero, "Distributed control of battery energy storage systems for voltage regulation in distribution networks with high PV penetration," *IEEE Transactions on Smart Grid*, vol. 9, no. 4, pp. 3582-3593, Jul. 2018.

[36] B. A. Robbins, C. N. Hadjicostis, and A. D. Domínguez-García, "A two-stage distributed architecture for voltage control in power distribution systems," *IEEE Transactions on Power Systems*, vol. 28, no. 2, pp. 1470-1482, May. 2013.

[37] X. Zhang, L. Wang, and B. Zhang *et al*., "Comprehensive configuration strategy of energy storage allocation and line upgrading for distribution networks considering a high proportion of integrated photovoltaics," *IET Energy System Integration*, vol. 5, no. 1, pp. 54-65, Mar. 2023.

[38] X. Cao, C. Gao, and D Li *et al*., "Mixed operation model of data network and power network and its participation in the economic operation of power system," *Proceedings of the IEEE*, vol. 38, no. 5, pp. 1448-1455, Mar. 2018.

[39] S. Chen, P. Li, and H. Ji *et al.,* "Operational flexibility of active distribution networks with the potential from data centers," *Applied Energy*, vol. 293, Jul. 2021.

[40] S. Wu, Q. Wang, and C. Miao, "Distribution network resilience enhancement strategy considering spatial-temporal migration of flexible resources on supply and demand sides," *IET Renewable Power Generation*, 1-16, Aug. 2023.

[41] Q. Yan, X. Dong, and J. Mu *et al*., "Optimal configuration of energy storage in an active distribution network based on improved multi-objective particle swarm optimization," *Power System Protection and Control*, vol. 50, no. 10, pp. 12-19, May 2022. (in Chinese)